

# Effect of Varying Curvature and Inter Element Spacing on Dielectric Coated Conformal Microstrip Antenna Array

Prasanna K. Singh\* and Jasmine Saini

**Abstract**—In the design of a conformal patch antenna array, a special care must be taken regarding the placement of elements and curvature bending. Presently, the authors try to explain the effect of these two factors on the key parameters such as return loss, mutual coupling, gain and directivity. Here, the analyses of parameters are done under the consideration of dielectric coated two-element antenna array model. This paper attempts to examine the characteristics of the dielectric coated conformal antenna array by varying its inter element spacing on the changing cylindrical geometry. The two-element conformal array is considered in  $E$ -plane and  $H$ -plane configurations, and its parameters are analyzed using full wave analysis and verified by HFSS tool. A comparative study shows that the  $E$ -plane configuration gives better result than  $H$ -plane configuration.

## 1. INTRODUCTION

The continuous intensive research and development work in the field of the conformal microstrip antenna array empowers the antenna to be more practically and commercially accepted. By optimizing its distinct features, these antennas will become a major driving factor in designing the futuristic singly or doubly curved communicating devices. The microstrip patch antennas mounted on a singly concave or convex curved surfaces such as circular cylinder geometry are an important class of applications where a wide area coverage or high directive beam is desirable [1, 2]. In some of the specific high end applications, the casing of a conformal antenna array is desirable, and here a dielectric material is considered as a protective layer. This coating influences the property of the antenna array due to the trapping or/and propagation of more energy along with the surface which increases the interactions between the antenna elements. Moreover, if there is a variation of either one or both the element bending and inter element spacing, then the antenna parameters deviate from their normal behavior [3–6]. This is due to the change in basic property of dielectric materials under bending strength and has a significant impact on fringing field and therefore; it affects the effective dielectric constant and hence affects the antenna parameters. So, it becomes exciting and inspiring to analyze the dielectric superstrate effect under the changing cylindrical radius with inter element spacing variations on the antenna array performances. Scant research has been observed in analyzing the dielectric coated rectangular microstrip patch antenna array conformal to the cylindrical surface for the Worldwide Interoperability for Microwave Access (WiMAX) application in the middle band typically at 3.5 GHz. This paper compares the two radiating elements by positioning them collinearly along the  $E$ -plane and  $H$ -plane configurations with simultaneous variations of cylindrical curvature typically from 1000 mm to nearly 100 mm radius and inter element separation from  $0.3\lambda$  to  $0.8\lambda$ . In Sections 2 and 3, the description and formulation of the antenna array model is discussed and expressed. The antenna parameters are calculated based on the method of moment technique and validated with the help of HFSS tool. The comparative tables and figures are depicted in Sections 4 and 5 for  $E$ - and  $H$ -plane antenna array configurations.

---

Received 20 February 2017, Accepted 15 May 2017, Scheduled 21 June 2017

\* Corresponding author: Prasanna Kumar Singh (singhprasanna25@yahoo.com).

The authors are with the Department of Electronics and Communication Engineering, Jaypee Institute of Information Technology, A10, Sector-62, Noida-201307, Uttar Pradesh, India.

## 2. SIGNIFICANCE OF INTER ELEMENT SPACING WITH DIELECTRIC LOADING ON CYLINDRICAL GEOMETRY

At present, two key factors are considered: (i) by varying inter-element distance and (ii) by changing the curvature of a cylindrical geometric platform for analyzing the dielectric loaded antenna array model. One of the important parameters is mutual coupling, which is due to the waves/fields that exist along the superstrate-antenna array interface [8, 9]. So, by selecting a correct distance, these fields can be decomposed to constructive space waves or destructive surface waves. The spacing at which one plane coupling overtakes the other also depends on the electrical properties and the geometrical dimensions of the microstrip antenna. Too large a spacing results in the presence of grating lobes, which are undesirable in most instances. On the other hand, too close a spacing leads to a broader beam width which may be unacceptable. To obtain maximum additive radiating fields, the separation between the elements should be about  $\lambda/2$ . In Figure 1(a), the two cylindrical rectangular patches show the coupling of two patches positioned in  $H$  and  $E$  plane configurations. Figure 1(b) shows that the side-by-side patches not only are a function of a relative alignment but also depend upon the radius of the curvature. When the elements are positioned collinearly along the  $E$ -plane, even for a small separation, the elements exhibit isolation, whereas when they are positioned collinearly in the  $H$ -plane, the separation has to be large for the same result. There is a considerable change in the overall behavior of the antenna during the transformation from planar to the non-planar surface. Figure 1 shows the cylindrical rectangular microstrip structures loaded with/without a protective dielectric layer as an example of the non-planar antenna model. Due to the varying of curvature radius, the dielectric material experiences mainly two types of effects, namely, 'stretching' and 'compression'. As a result of the superstrate effect, the overall effective dielectric constant of the model is increased, and hence the change in fringing field is observed. Consequently, some of the antenna parameters, such as resonance frequency, quality factor, input impedance, voltage standing wave ratio, return loss, and antenna bandwidth, are the functions of curvature. In particular, due to the dielectric coating on the antennas, the resonance frequency of an antenna changes, and the corresponding fractional change in resonance frequency is calculated using [7].

$$\frac{\Delta F_r}{F_r} = \frac{1}{2} \frac{\frac{\Delta \epsilon_e}{\epsilon_{e0}}}{1 + \frac{1}{2} \frac{\Delta \epsilon_e}{\epsilon_{e0}}} \quad (1)$$

where,  $\epsilon_{e0}$  = effective dielectric constant without coating,  $\Delta \epsilon_e$  = change in effective dielectric constant due to coating,  $\Delta F_r$  = fractional change in resonant frequency, and  $F_r$  = resonant frequency.

Additionally, the antenna performance will be dependent on the type and thickness of dielectric materials used as a substrate and superstrate and their bending angle [3]. In the present case, the

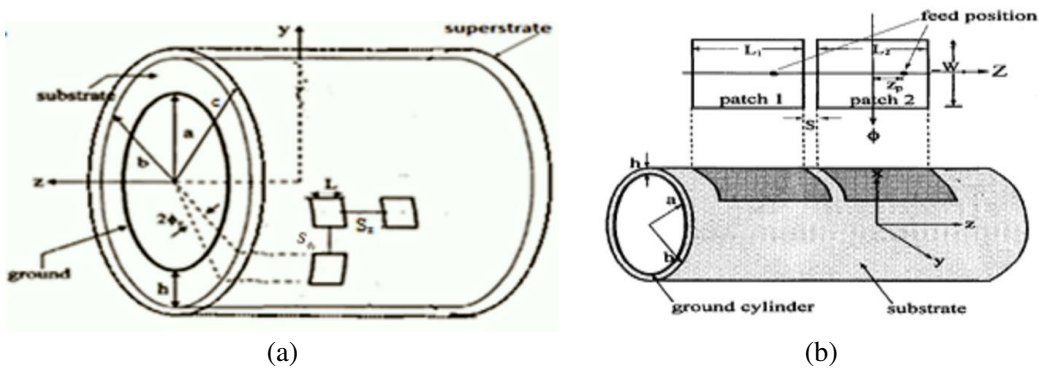


**Figure 1.** (a) Two element cylindrical rectangular patch antenna array arranged in  $H$ -plane and  $E$ -plane configuration. (b) Two rectangular microstrip antenna array mounted on a convex structure with gap coupled.

calculation of enhanced effective permittivity  $\varepsilon_{r,eff}$  [8] is extended and given by

$$\varepsilon_{r,eff} = \varepsilon_{r1}p_1 + \varepsilon_{r1}^2(1-p_1)^2 * [\varepsilon_{r1}p_2p_3 + \{p_2p_4 + (p_3 + p_4)^2\}] * [\varepsilon_{r1}p_2p_3p_4 + (\varepsilon_{r1}p_3 + p_4)(1-p_1-p_4)^2 + p_4\{p_2p_4 + (p_3 + p_4)^2\}]^{-1} \quad (2)$$

where,

$$\begin{aligned} p_1 &= 1 - \frac{h_1}{2w_e} \ln \left( \frac{\pi}{h_1} w_e - 1 \right) - p_4 \\ p_2 &= 1 - p_1 - p_3 - 2p_4 \\ p_3 &= \frac{h_1 - g}{2w_e} \ln \left[ \frac{\pi w_e}{h_1} \frac{\cos \left[ \frac{\pi g}{2h_1} \right]}{\pi \left( 0.5 + \frac{h_2}{h_1} \right) + \frac{0.5g\pi}{h_2}} + \sin \left( \frac{0.5g\pi}{h_1} \right) \right] \\ p_4 &= \frac{h_1}{2w_e} \ln \left( \frac{\pi}{2} - \frac{h_1}{2w_e} \right) \\ g &= \frac{2h_1}{\pi} \cdot \arctan \left[ \frac{\frac{\pi h_2}{h_1}}{\left( \frac{\pi}{2} \right) \left( \frac{w_e}{h_1} \right) - 2} \right] \\ w_e &= \sqrt{\frac{\varepsilon_{r1}}{\varepsilon'_r}} \left[ \left\{ w + 0.882h_1 + 0.1644h_1 \frac{(\varepsilon'_r - 1)}{(\varepsilon'_r)^2} \right\} + h_1 \frac{(\varepsilon'_r + 1)}{\pi \varepsilon'_r} \left\{ \ln \left( 0.94 + \frac{w}{2h_1} \right) + 1.451 \right\} \right] \\ \varepsilon'_r &= \frac{2\varepsilon_{r1} - 1 + \left( 1 + \frac{10h_1}{w_e} \right)^{-1/2}}{1 + \left( 1 + \frac{10h_1}{w_e} \right)^{-1/2}} \end{aligned} \quad (3)$$

where,  $h_1$  and  $h_2$  are the thickness of substrate and superstrate, respectively ( $h_1 = h_2$ ), and  $\varepsilon_{r1}$  is the relative permittivity of substrate/superstrate material.

### 3. ANTENNA ARRAY MODEL

Referring to the geometry shown in Figure 1, the dielectric coated two elements rectangular microstrip antenna array is flush mounted on a conducting circular cylinder, which represents an important class of conformal antennas. The cylindrical substrate and superstrate are of the same thickness  $h_1 = h_2$  ( $b - a = c - b$ ) and have similar relative permittivities and permeabilities  $\mu_0$ . The antenna array is at  $\rho = b$ , and each has dimensions of  $(2L \times 2b\phi_0)$ , where  $2L$  is the straight dimension and  $2\phi_0$  the angle subtended by the curved element in the microstrip array. All the elements in the array have the same measurement and assumed to be uniformly excited. The array is placed between the substrate and superstrate layers, and the inter-element spacing,  $S(S_z = S\phi_0)$ , is variable in the  $z$  and  $\phi$  directions and curvature variation in  $\rho$  direction. The assumption that the cylinder is infinite in the axial  $z$ -direction reduces the three-dimensional problem to a one-dimensional one, if the fields and currents are expressed in the spectral domain. The analysis of dielectric coated two element rectangular inset-fed patches mounted on a singly curved or circular cylindrical perfect electric conductor (PEC) structure is treated by applying the moment method in the spectral domain. Consider the  $TM_{mn}$  mode as exciting mode, since the thickness of the dielectric material is much smaller than that of the operating wavelength. The outer region ( $\rho > c$ ) is a free space with permeability  $\mu_0$  and permittivity  $\epsilon_0$ . By considering these assumptions, the two elements radiator can be substituted by the surface current dissemination and by employing the boundary conditions at the interface, the total electric field tangential to the array surface must be zero which is applied to the present case; hence on the antennas,

$$\hat{\rho} \times [E^P(\phi, z) + E^F(\phi, z)] = 0 \quad (4)$$

where,  $E^P(\phi, z)$  is the electric field due to the patch current and  $E^F(\phi, z)$  the electric field due to the feed with the patch being absent. These unknown parameters need to be solved, and then the input impedance, radiation pattern, etc. can be calculated [1, 3]. The close proximity between the patch and the ground plane suggests that for a cylindrical microstrip structure, the electric field has only a  $\hat{\rho}$  component, and the magnetic field has only  $\hat{\phi}$  and  $\hat{z}$  components in the region bounded by the patch and the ground cylinder. The resonant frequencies of the  $TM_{mn}$  mode for the rectangular cylindrical antennas is given by

$$(F_r)_{mn} = \frac{c}{2\sqrt{\varepsilon_{r,eff}}} \sqrt{\left[\frac{m}{2\phi_0\rho}\right]^2 + \left[\frac{n}{2L}\right]^2} \quad (5)$$

where,  $c$  is the speed of light in the presence of dielectric non-magnetic media, and  $\varepsilon_{r,eff}$  is the overall effective permittivity due to superstrate and substrate materials and is calculated from Eq. (2).

The full-wave solutions can be obtained by numerical convergence for the moment-method calculation. The numerical convergence strongly depends on the basis function chosen for the expansion of the patch surface current density.

The two patches are fed at  $(\phi_{f1}, z_{f1})$  and  $(\phi_{f2}, z_{f2})$ , respectively, and are of the same dimension. The feed is modeled as a line source with a unit amplitude current density given as

$$J_p^{(i)} = \frac{\hat{\rho}\delta(\phi' - \phi_{pi})\delta(z' - z)}{\rho'}, \quad a \leq \rho' \leq b, \quad i = 1, 2 \quad (6)$$

where the superscript  $i$  denotes the source current at antenna  $i$ . The given antenna systems is modeled as a two-port network with a  $2 \times 2$  port impedance matrix  $[Z_P]$ . The relation between the port voltages and currents is defined as

$$\begin{bmatrix} V_1^P \\ V_2^P \end{bmatrix} = \begin{bmatrix} Z_{11}^P & Z_{12}^P \\ Z_{21}^P & Z_{22}^P \end{bmatrix} \begin{bmatrix} I_1^P \\ I_2^P \end{bmatrix} \quad (7)$$

where, the superscript  $p$  denotes the port quantities. To determine the port impedance matrix, the input impedance  $[Z_{11}^P]$  of the excited antenna with the presence of the other antenna open-circuited and the mutual impedance  $[Z_{12}^P]$  between the two antennas must be calculated.

For a two-port network shown in Figure 2, the scattering matrix  $[S]$  can be evaluated from

$$[S] = \frac{[Z^P] - Z_0[U]}{[Z^P] + Z_0[U]} \quad (8)$$

where  $[U]$  is a unit matrix of order  $2 \times 2$ , and  $Z_0$  is the characteristic impedance of the inset feeding (assumed to be  $50\Omega$  here). To solve  $[Z_{11}^P]$  and  $[Z_{12}^P]$ , the full-wave analysis and Galerkin's moment-

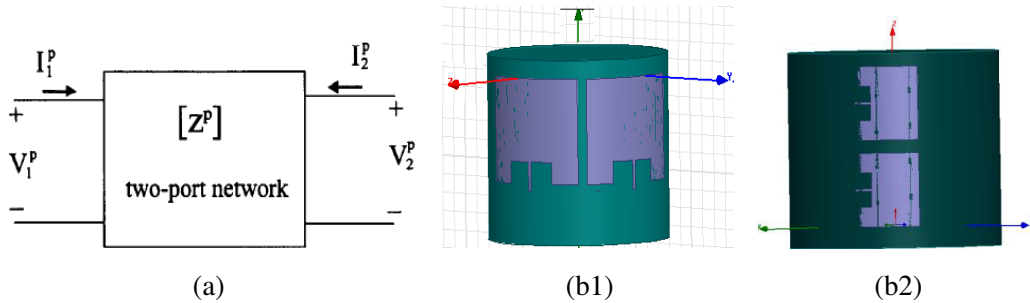


**Figure 2.** (a) Two coupled rectangular patch antennas using two port network model. (b) Cylindrical rectangular patch antenna model in (b1)  $H$ -plane configuration, (b2)  $E$ -plane configuration.

method technique [1] can be used:

$$Z_{11}^p = - \int_a^c E_\rho^{(1)}(\rho, \phi_1, z_1) d\rho \tag{9}$$

$$Z_{21}^p = - \int_a^c E_\rho^{(1)}(\rho, \phi_2, z_2) d\rho \tag{10}$$

with

$$E_\rho^{(1)}(\rho, \phi_i, z_i) = \frac{1}{2\pi} \sum_{n=-\infty}^{\infty} e^{jn\phi_i} \int_{-\infty}^{\infty} dk_z e^{jk_z z_i} \overset{\cong T}{G}_\rho(n, k_z) \begin{bmatrix} \tilde{J}_\phi^{(i)}(n, k_z) \\ \tilde{J}_z^{(i)}(n, k_z) \end{bmatrix}, \quad i = 1, 2, \tag{11}$$

where  $\overset{\cong T}{G}_\rho(n, k_z)$  relates the  $\hat{\rho}$  component of the spectral domain electric field inside the substrate layer to the patch surface current densities  $\tilde{J}_z^{(i)}$  and  $\tilde{J}_\phi^{(i)}$  of the patch. These unknown variables can be defined and calculated [1]. From Eqs. (8) and (9),  $[Z_{11}^p]$ , and  $[Z_{21}^p]$  are determined respectively, and the mutual coupling coefficient can be calculated from Eq. (8) and given as

$$S_{21} = 2Z_{21}^p \frac{Z_0}{(Z_{11} + Z_0)^2 - (Z_{21}^p)^2} \tag{12}$$

where,  $Z_0$  is assumed to be 50 ohm.

**Table 1.** The performance analysis of the antenna model in  $H$ -plane configuration at radius = 100 mm.

Inter element spacing	Calculated Antenna Parameters					Simulated Antenna Parameters				
	$F_r$ (GHz)	$S_{11}$ (dB)	$S_{21}$ (dB)	Gain (dB)	Directivity (dB)	$F_r$ (GHz)	$S_{11}$ (dB)	$S_{21}$ (dB)	Gain (dB)	Directivity (dB)
0.3λ	7.9	-17.3	-28.2	2.1	2.5	7.4	-17.1	-27.5	2.1	2.4
0.4λ	8.1	-18.7	-28.2	2.1	2.5	7.9	-17.9	-27.8	2.3	2.4
0.5λ	8.4	-20.1	-28.7	2.1	2.6	7.9	-18.4	-28.1	2.3	2.4
0.6λ	8.4	-22.5	-28.7	2.2	2.6	8.1	-19.8	-28.4	2.2	2.5
0.7λ	8.5	-22.3	-29.1	2.3	2.7	8.3	-21.7	29	2.1	2.6
0.8λ	8.4	-20.1	-29.2	2.2	2.8	8.3	-20	-28.9	2.1	2.6

**Table 2.** The performance analysis of the antenna model in  $H$ -plane configuration at radius = 500 mm.

Inter element spacing	Calculated Antenna Parameters					Simulated Antenna Parameters				
	$F_r$ (GHz)	$S_{11}$ (dB)	$S_{21}$ (dB)	Gain (dB)	Directivity (dB)	$F_r$ (GHz)	$S_{11}$ (dB)	$S_{21}$ (dB)	Gain (dB)	Directivity (dB)
0.3λ	7.7	-14.1	-25.7	1.8	2.3	7.5	-14	-25.4	1.6	2.2
0.4λ	7.7	-14.1	-25.7	1.8	2.4	7.5	-14.1	-25.6	1.6	2.2
0.5λ	7.8	-14.4	-26.1	1.9	2.4	7.6	-14.1	-25.9	1.7	2.2
0.6λ	7.8	-14.3	-27	2	2.4	7.6	-14.2	-26.5	1.7	2.3
0.7λ	7.9	-15.7	-27.1	1.9	2.4	7.8	-15.6	-26.9	1.7	2.4
0.8λ	7.8	-14.7	-27	1.9	2.3	7.6	-14.6	-26.8	1.6	2.3

#### 4. DESIGN DESCRIPTION

The antenna array model shown in Figure 2(b) is only valid for the flexible dielectric materials with small thickness and low relative permittivity with nonmagnetic property. All the metal surfaces are assumed to be perfect electric conductors (PEC) with minimal thickness compared to the wavelength. The rectangular microstrip antenna array is mounted on an RT Duroid 5880 between a substrate and superstrate of the same thickness ( $h_1 = h_2$ ) 5 mils with relative permittivity 2.3, which can be easily made conformal to cylindrical ground surfaces of different radii. The calculated overall enhanced permittivity of the model is approximately 2.37. The air is in outermost region, which is free-space with permittivity  $\epsilon_0$  and permeability  $\mu_0$ . In order to achieve the impedance matching condition, the input impedance of the antenna model at various cylinder radii and spacings, the inset feed is adjusted to  $50\ \Omega$  at the  $TM_{01}$  mode excitation. The mutual coupling coefficient  $S_{12}$  is measured as a function of edge spacing between two patch antennas, as well as the cylindrical radii. MATLAB is used for finding antenna dimensions and its parameters at an operating frequency 3.5 GHz [1, 9, 10]. The HFSS tool is then applied to dimension optimization, patch antenna dimension ( $28.52\ \text{mm} \times 33.86\ \text{mm}$ ), and validation. The results are first tested for the planar surface, and then it is transformed into the non-planar surface at different radii which vary from 1000 mm to 100 mm with inter element separation  $S(S_z = S\phi_0)$  from  $0.3\lambda$  to  $0.8\lambda$  respectively. The different cases are discussed in Table 1, Table 2 and Table 3, respectively, for the  $H$ -plane antenna model configuration by varying their radius and inter-element spacing. Also, the performances of the  $E$ -plane antenna model are analyzed at various radii and inter-element spacings which tabulated in Table 4, Table 5 and Table 6, respectively. The comparative study shows that the theoretical and simulated antenna parameters are analogous and desirable. Moreover, it has been observed that the  $E$ -plane results are better than the  $H$ -plane configuration antenna model. Generally, the antenna parameters at  $0.7\lambda$  inter element spacing are better than the other inter element spacing values. Hence, for an instance, the plots of these results at radius 500 mm are shown in Figures 3 and 4.

**Table 3.** The performance analysis of the antenna model in  $H$ -plane configuration at radius = 1000 mm.

Inter element spacing	Calculated Antenna Parameters					Simulated Antenna Parameters				
	$F_r$ (GHz)	$S_{11}$ (dB)	$S_{21}$ (dB)	Gain (dB)	Directivity (dB)	$F_r$ (GHz)	$S_{11}$ (dB)	$S_{21}$ (dB)	Gain (dB)	Directivity (dB)
$0.3\lambda$	5.5	-14.5	-18.7	1.7	2.3	5	-14.1	-18.9	1.6	2.2
$0.4\lambda$	5	-14.8	-19.1	1.8	2.4	4.8	-14.3	-19.1	1.6	2.3
$0.5\lambda$	4.9	-15.5	-19.4	1.7	2.4	4.7	-15.1	-19.2	1.5	2.3
$0.6\lambda$	4.9	-15.8	-19.6	1.7	2.4	4.7	-15.3	-19.2	1.5	2.3
$0.7\lambda$	4.8	-15.8	-19.4	1.8	2.3	4.7	-15.3	-19.1	1.6	2.3
$0.8\lambda$	4.8	-15.7	-18.9	1.8	2.3	4.5	-15.4	-18.5	1.5	2.2

#### 5. OBSERVATIONS AND DISCUSSIONS

In the previous section, it has been observed that the antenna parameters are dependent on the model physical geometry, and the relationship between antenna parameters and model physical geometry is depicted in Figures 3 and 4 for a particular case as an example. The isolated mutual coupling due to two elements is measured in terms of three factors, namely, frequency, inter element spacing and curvature of the platform. Here, the dielectric coating acts as a protective layer in such a way that it does create a moderate hindrance and satisfies the purposes. From the observation tables, it is also found that for a large edge spacing, the coupling decreases more rapidly with increasing cylinder radius. This is probably because for fixed edge spacing, the two patches on a cylindrical body with smaller radius are subtended

**Table 4.** The performance analysis of the antenna model in *E*-plane configuration at radius = 100 mm.

Inter element spacing	Calculated Antenna Parameters					Simulated Antenna Parameters				
	$F_r$ (GHz)	$S_{11}$ (dB)	$S_{21}$ (dB)	Gain (dB)	Directivity (dB)	$F_r$ (GHz)	$S_{11}$ (dB)	$S_{21}$ (dB)	Gain (dB)	Directivity (dB)
0.3 $\lambda$	8	-28	-35	1.9	4.3	7.9	-27.8	-34.9	1.9	4.1
0.4 $\lambda$	8.1	-28.7	-37	2.1	4.3	7.8	-28.1	-36.8	2.1	4.2
0.5 $\lambda$	8.2	-29	-38	2.1	4.2	8.1	-28.8	-37.5	2.2	4.0
0.6 $\lambda$	8.3	-30	-38	2.1	4.2	8.2	-29.7	-37.8	2	4.1
0.7 $\lambda$	8.3	-31	-40	2.2	4.2	8.1	-30.8	-39.5	2	4.1
0.8 $\lambda$	8.4	-29	-39	2.2	4.3	8.2	-28.9	38.6	2	4.1

**Table 5.** The performance analysis of the antenna model in *E*-plane configuration at radius = 500 mm.

Inter element spacing	Calculated Antenna Parameters					Simulated Antenna Parameters				
	$F_r$ (GHz)	$S_{11}$ (dB)	$S_{21}$ (dB)	Gain (dB)	Directivity (dB)	$F_r$ (GHz)	$S_{11}$ (dB)	$S_{21}$ (dB)	Gain (dB)	Directivity (dB)
0.3 $\lambda$	7	-20	-28.3	2.1	4.5	6.8	-19.2	-27.8	2.1	4.4
0.4 $\lambda$	7.1	-20.1	-28.7	2.1	4.5	6.8	-19.5	-28.2	2	4.4
0.5 $\lambda$	7.1	-20.5	-28.7	2.1	4.6	6.9	-19.9	-28.5	2.1	4.5
0.6 $\lambda$	7.1	-21.1	-28.9	2	4.6	7.1	-20.5	-28.6	1.9	4.5
0.7 $\lambda$	7	-20.2	-28.8	2.1	4.7	7.1	-20.1	-28.8	1.9	4.6
0.8 $\lambda$	7.1	-20	-28.8	2.1	4.7	6.9	-19.7	-28.7	2	4.6

**Table 6.** The performance analysis of the antenna model in *E*-plane configuration at radius = 1000 mm.

Inter element spacing	Calculated Antenna Parameters					Simulated Antenna Parameters				
	$F_r$ (GHz)	$S_{11}$ (dB)	$S_{21}$ (dB)	Gain (dB)	Directivity (dB)	$F_r$ (GHz)	$S_{11}$ (dB)	$S_{21}$ (dB)	Gain (dB)	Directivity (dB)
0.3 $\lambda$	6	-15.5	-26.1	1.9	4.6	5.5	-15.2	-25.7	1.7	4.5
0.4 $\lambda$	5.7	-15.7	-26.1	1.9	4.6	5.4	-15.4	-25.8	1.6	4.5
0.5 $\lambda$	5.7	-15.8	-26.2	1.8	4.7	5.4	-15.5	-26.0	1.6	4.6
0.6 $\lambda$	5.9	-15.8	-26.2	1.8	4.7	5.5	-15.5	-26.1	1.7	4.6
0.7 $\lambda$	6	-15.9	-26.2	1.8	4.6	5.6	-15.6	-26.2	1.7	4.5
0.8 $\lambda$	6	-15.8	-26.1	1.8	4.6	5.6	-15.5	-25.8	1.6	4.5

by a large angle, which results in attenuation of the space wave. In this case, the two patches are on opposite sides of the cylindrical host, which results in a minimal coupling level. However, the coating has a significant effect on the array mutual coupling, but due to small thickness of superstrate/substrate the mutual coupling has minimal influence under sufficient bending of the model. The coating effect becomes more pronounced at higher frequencies where the coating becomes electrically thicker.

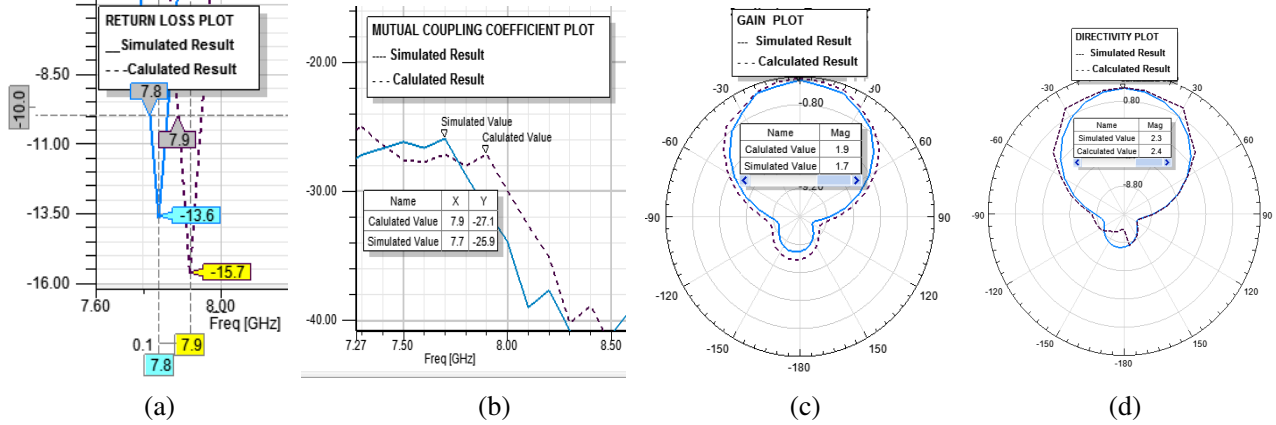


**Figure 3.** *H*-plane configuration performance comparison plot between calculated results and simulated results for radius = 500 mm at  $0.7\lambda$  inter-element spacing for (a) return loss, (b) mutual coupling coefficient, (c) gain, (d) directivity.

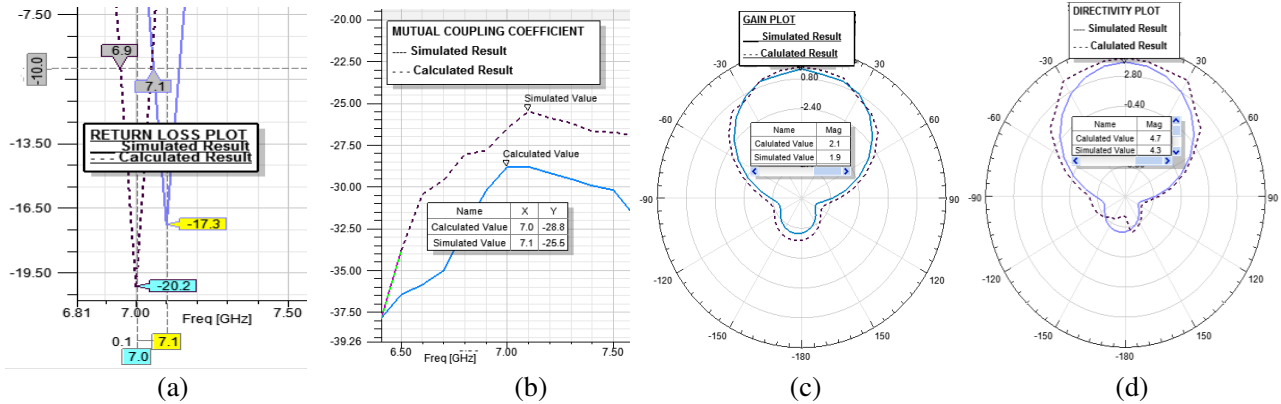


**Figure 4.** *E*-plane configuration performance comparison plot between calculated results and simulated results for radius = 500 mm at  $0.7\lambda$  inter-element spacing for (a) return loss, (b) mutual coupling coefficient, (c) gain, (d) directivity.

### 6. CONCLUSIONS

In this antenna array model, the effect of changing circular cylindrical bending with varying inter-element spacing is dealt with very carefully, and the contributions of these many changes to the antenna parameters are also studied. The full-wave analysis method is used for finding the calculated results which are in good agreement with the simulated ones. Here, a simple and novel approach is adopted, and it is a unique one under this specifications and application. As expected, the resonant frequency shifts towards the upper band of WiMax as bending of the model increases. In the convex structure platform, the mutual coupling coefficient also gives better results as the structure is bent more and by incrementing the separation. Also, the gain and directivity values do not change very much, and their performances can be improved by considering larger number of elements in the array. The mutual coupling can be further reduced by simply using thinner dielectric material which will result in less surface-wave excitation. These observations will guide us in designing the efficient model and predicting their performance for a particular range of applications. The designing of such a conformal patch antenna array with wide angle scanning feature requires a large number of antenna elements, which is a challenging task for a portable device. For further extension, this approach can also be readily extended to multi-layers conformal patch antenna which shall be reported in due course of time.

**REFERENCES**

1. Wong, K.-L., *Design of Nonplanar Microstrip Antennas and Transmission Lines*, 16–30, John Wiley & Sons Inc., New York, 1999.
2. Josefsson, L. and P. Persson, *Conformal Array Antenna Theory and Design*, 155–258, John Wiley & Sons Inc., New Jersey, 2006.
3. Singh, P. K. and J. Saini, “Performance analysis of superstrate loaded cylindrically conformal microstrip antenna on the varying curvature for Wimax applications,” *International Journal of Microwave and Optical Technology*, Vol. 11, No. 6, 406–412, Nov. 2016.
4. Alexopoulos, N. G. and D. R. Jackson, “Fundamental superstrate (cover) effect on printed circuit antennas,” *IEEE Transactions on Antennas and Propagation*, Vol. 32, 807–816, 1984.
5. You, C., W. Hwang, and M. Tenteris, “Impact behavior and radiation performance of a structurally integrated antenna array conformed around cylindrical bodies,” *IEEE International Symp. Antennas and Propag. Soc.*, 3844–3847, Jun. 2007.
6. Tam, W. Y., A. K. Y. Lai, and K. M. Luk, “Mutual coupling between cylindrical rectangular microstrip antennas,” *IEEE Transactions on Antennas and Propagation*, Vol. 43, No. 8, 897–899, Aug. 1995.
7. Krowne, C. M., “Cylindrical-rectangular microstrip antenna,” *IEEE Transactions on Antennas and Propagation*, Vol. 31, No. 1, 194–199, Jan. 1983.
8. Guha, D. and J. Y. Siddiqui, “Resonant frequency of circular microstrip antenna covered with dielectric superstrate,” *IEEE Transactions on Antennas and Propagation*, Vol. 51, No. 7, 1649–1652, Jul. 2003.
9. Balanis, C. A., *Antenna Theory, Analysis and Design*, 3rd Edition, 811–876, John Wiley & sons, New York, 2005.
10. Zhang, K. and D. Li, *Electromagnetic Theory for Microwaves and Optoelectronics*, 2nd Edition, 117–178, Springer-Berlin Heidelberg, New York, 1998.